BEND STRESS RELAXATION AND TENSILE PRIMARY CREEP OF A POLYCRYSTALLINE α-SiC FIBER

Gregory N. Morscher[1], Hee Man Yun[2], and Jon C. Goldsby[3]

[1]Case Western Reserve University, Cleveland, OH
[2]Cleveland State University, Cleveland, OH
[3]NASA Lewis Research Center, Cleveland, OH

INTRODUCTION

Understanding the thermomechanical behavior (creep and stress relaxation) of ceramic fibers is of both practical and basic interest. On the practical level, ceramic fibers are the reinforcement for ceramic matrix composites which are being developed for use in high temperature applications. Some uses of structural ceramic matrix composites require that the continuous ceramic fibers display creep strain tolerances of less than 1% and sometimes as low as 0.1% for long time service (Dicarlo, 1994). For this reason it is important to understand and model the total creep of fibers at low strain levels where creep is predominantly in the primary stage. In addition, there are many applications where the component will only be subjected to thermal strains. Therefore, the stress relaxation of composite consituents in such circumstances will be an important factor in composite design and performance controlling for example, the distribution of residual stress.

On the basic level, ceramic fibers are high aspect ratio monolithic ceramics which can be used for performing creep, relaxation, and recovery experiments. Since ceramic fibers are usually stronger than bulk specimens, higher stresses can be applied to a fiber in tension resulting in wider stress ranges for determining creep stress exponents and thus more critical tests for models of creep at low strain levels. Also, since ceramic fibers can be bent relatively easily, the comparison of deformation in tension and pure bending can be examined.

The objective of this paper is to compare and analyze bend stress relaxation and tensile creep data for α-SiC fibers produced by the Carborundum Co. (Niagara Falls, NY). This fiber is of current technical interest and is similar in composition to bulk α-SiC which has been studied under compressive creep conditions (Lane et al.,1988, Nixon and Davis, 1992). The temperature, time, and stress dependences will be discussed for the stress relaxation and creep results. In addition, some creep and relaxation recovery experiments were performed in order to understand the complete viscoelastic behavior, i.e. both recoverable and nonrecoverable creep components of these materials. The data will be presented in order to model the deformation behavior and compare relaxation and/or creep behavior for relatively low deformation strain conditions of practical concern. Where applicable, the tensile creep results will be compared to bend stress relaxation data.

Plastic Deformation of Ceramics, Edited by
R.C. Bradt *et al.*, Plenum Press, New York, 1995

BEND STRESS RELAXATION TESTING

A simple test developed to determine the creep properties of ceramic fibers is the bend stress relaxation (BSR) test (Fig. 1); this technique has been described in detail by Morscher and DiCarlo (1992). For this study, the test procedure was as follows: fibers were placed in graphite mandrels of known radius R_o, i.e. a constant bend strain. The

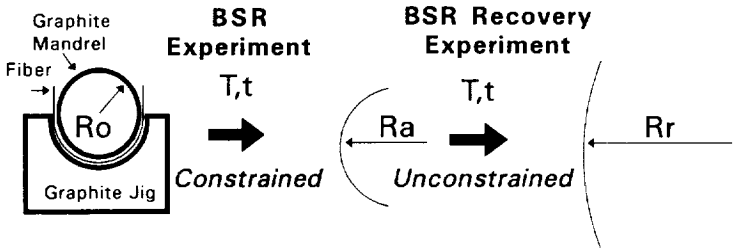

Figure 1. Schematic representation of bend stress relaxation and bend stress relaxation recovery experiments.

constrained fibers were then subjected to a heat treatment at temperature, T, for 1, 10, or 100 hours in argon. After cooling the fibers were removed from the fixture and the radius of curvature, R_a, was measured. The amount of relaxation was quantified by the stress relaxation ratio m (1) which gives the ratio of the remaining elastic stress in the fiber, $\sigma_e(t,T)$, to the initial applied elastic stress, $\sigma_e(0,T)$,

$$m = \sigma_e(t,T)/\sigma_e(0,T) = 1 - R_o/R_a \qquad (1)$$

imposed by the radius R_o. If m = 1, the fibers behaved elastically and did not relax, if m < 1 then some relaxation occurred and if m = 0 then full relaxation occurred (i.e. treated fibers retained the constrained radius R_o). BSR tests were performed to determine the temperature, time, and applied strain dependence for m.

BSR strain "recovery" experiments (Fig. 1) were performed by placing bent (from BSR experiments) fibers and subjecting them to heat treatments in argon without constraint. Fibers were either placed in grafoil envelopes or supported by one end in holes drilled into a graphite block so that the fibers were free to move. Heat treatments ranged from approximately the same time-temperature conditions as the BSR treatment to temperatures 200°C higher and/or 2 orders of magnitude longer times than the BSR condition. The remaining radius of curvature, R_r, was then measured after the recovery experiment.

TENSILE CREEP TESTING

The details of the tensile creep rigs and procedures are described elsewhere (Yun et al. 1994, Goldsby et al., 1994). Creep tests were performed in air ($MoSi_2$ heating elements) or vacuum (carbon heating elements). All creep tests were dead weight loaded and displacement was measured with an LVDT. Fibers extended out of the hot zone and were mounted with epoxy to paper tabs (i.e. a "cold grip" test). The hot zones were determined to be 75 mm for air and 93 mm for vacuum experiments from the furnace temperature profiles. For the air experiments, the load was applied to the fiber 10 minutes after the desired temperature was reached. For the vacuum experiments, the load was

applied at room temperature and the furnace was heated up rapidly (100 °C/min) to the test temperature. At different times during the vacuum experiments the temperature would be brought back to room temperature to measure the creep-induced displacement. The furnace would then again be rapidly heated to the test temperature and the creep experiment continued. This exercise was performed in order to more accurately measure the "total"creep strain and it provided a check of the consistency of the displacement measure at high temperatures.

Creep recovery experiments were performed in tension after some air and vacuum creep experiments. For air experiments, the load was removed* at temperature whereas for vacuum experiments, the load was removed at room temperature and the sample was quickly heated up to the original creep temperature. Creep recovery experiments were performed for times ranging from the same time as tensile creep up to 30 times the time for tensile creep.

FIBERS TESTED

The α-SiC fiber (Frechette et al., 1991) used in this study was produced by sintering at temperatures above 2000°C. The fiber diameter is approximately 33 $\pm$ 2 μm and the grain size is approximately 2 μm $\pm$ 1 μm (Fig. 2a). The fiber does contain some boron and carbon which is in the form B_4C precipitates within the SiC grains and graphite grains (Giannuzzi, 1994). The fiber does have some porosity (at least 2%) and the fiber modulus is assumed to be 400 GPa

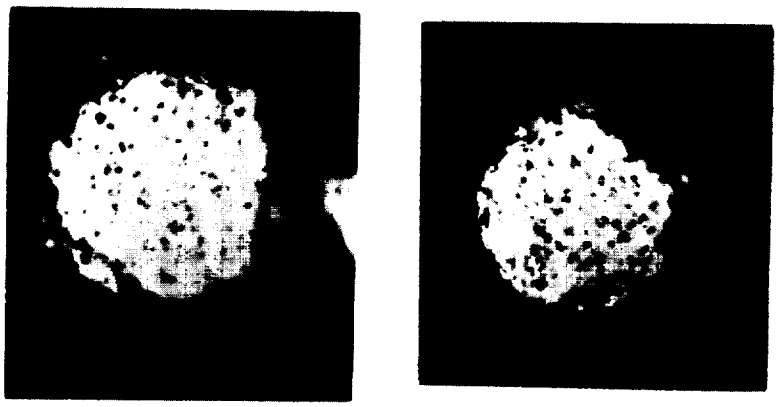

Figure 2. Optical micrographs of the cross-section of α-SiC fibers: (a) as-produced and (b) after creep (1535°C, 103 MPa, 15 h.) and recovery (1535°C; air; 44 hours).

RESULTS AND ANALYSIS

Bend Stress Relaxation

The effect of bend strain on m is shown in Fig. 3 for a number of BSR experiments performed with two different bend radii (25.4 and 8 mm). There appears to be only a

* For tensile recovery experiments, the fiber was still loaded (~ 15 MPa) with the LVDT core and epoxy tab.

small dependence of bend strain on m; therefore, the time and temperature dependence of stress relaxation was compared for the same bend radius (8 mm). The time-temperature effects on m are shown for 1, 10, and 100 hour experiments as a function of reciprocal temperature in Fig. 4. There is appreciable scatter in some experiments, e.g. m can vary by $\pm$ 0.04 (Fig. 3) some of this can be attributed to different diameter fibers and fibers not exactly aligned in the BSR jig. However, the degree of scatter from the material itself is not known, but is probably not zero. The relaxation data appears to be thermorheologically simple, that is the m data could be represented on a single curve by displacing the 10 and 100 hour data by a factor $\Delta(1/T)$ and 2 $\Delta(1/T)$, respectively (not shown). The best fit $\Delta(1/T)$ spacing corresponds to an apparent activation energy (described below), Q, of 850 $\pm$ 50 kJ/mol from the cross-cut method (Damask and Dienes, 1963).

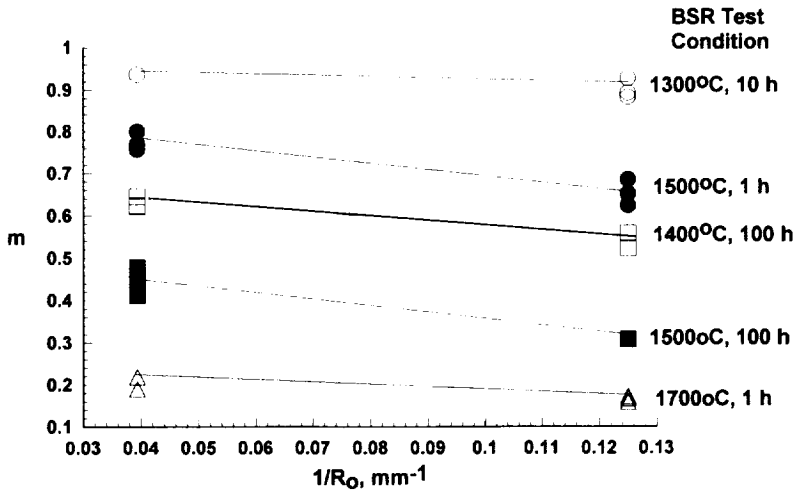

Figure 3. The effect of the applied bend radius on stress relaxation ratio m for several BSR test conditions.

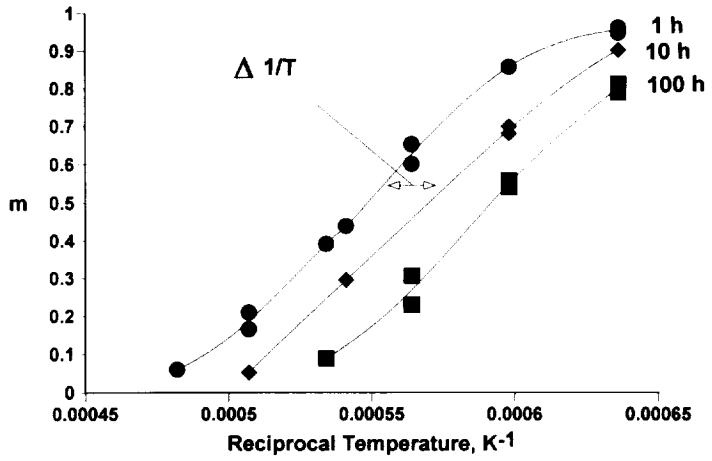

Figure 4. Temperature dependence of the BSR m ratio for 1, 10, and 100 hour tests. Each data point represents the average of 2 to 4 fibers.

Tensile Creep

Tensile creep was performed between 1400 and 1535°C in air and between 1420 and 1600°C in vacuum. Typical creep curves are shown in Fig. 5. It appears for all of the test conditions of this study, a steady state creep regime was never reached. At constant temperature, a time power law can be used to describe the creep strain, $\varepsilon_c = At^p$, where A

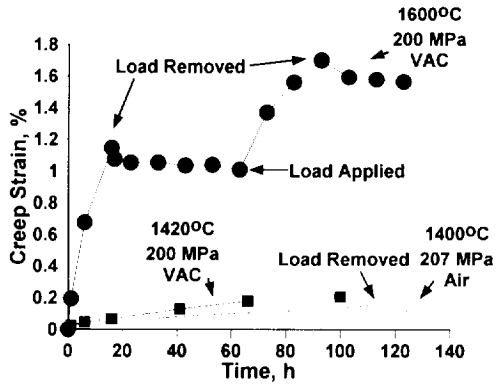

Figure 5. Typical tensile creep and recovery curves. The elastic strain is not shown before or after the load was applied or removed, i.e. all the strain shown is time dependent. The vacuum datapoints are from displacement measurements at room temperature during the experiments.

is a creep constant for a given temperature and stress, t is the time, and p is the time exponent (Table I). To determine a stress dependence of A, the creep strain measured in air after 20 hours at 1400°C and after 5 hours at 1535°C are plotted versus stress in Fig. 6. There appears to be a stress dependence of $n = 1.1 \pm 0.1$ (determined from linear regression analysis of $\ln \varepsilon_c$ vs σ from Fig. 6) for $\varepsilon_c \propto \sigma^n$. The tensile creep strain is plotted versus time on log/log scales in Fig. 7a and 7b for 138 and 207 MPa creep experiments in air and 200 MPa experiments in vacuum, respectively. The time dependence was obtained from linear regression of $\ln(\varepsilon_c)$ vs $\ln(t)$ for the specific creep experiments that are given in Table 1.

There appears to be a greater time dependence for 1535°C tensile creep in air than 1400°C tensile creep in air (Fig. 7a) due to oxidation. Because the time exponent is nearly constant during vacuum creep testing between 1420 and 1600oC (Fig. 7b), it is possible that the increase in p during air testing is due to the oxidation of the fiber, i.e. a reduction in the diameter of the SiC and an increase in the applied stress over time at temperature. Evidence of this is shown in Fig. 2b: a 1535°C crept and recovered fiber (total time at 1535°C was 44.4 hours) with a SiO_2 scale of ~ 3 μm.

To determine the temperature dependence, the creep strain for 200 MPa creep experiments was plotted verses reciprocal temperature in Fig. 8 for 1, 10, and 100 hours. Only the vacuum data were used since a wider temperature range and longer times were available. The $\Delta(1/T)$ spacing between 1, 10, and 100 hours curves was determined by displacing the 10 and 100 hour data to the 1 hour and best fitting $\Delta(1/T)$ by a linear regression technique (DiCarlo and Morscher, 1991). The $\Delta(1/T)$ spacing corresponds to an apparent activation energy by the relationship $Q = 2.3R/\{\Delta(1/T)\}$, where $Q = 750 \pm$

100 kJ/mol. This approach of determining activation energy is similar to the analysis of Sherby and Dorn, (1952) and Sherby et al (1954) for primary creep of metals.

Table 1. Experimental creep results and best fit creep parameters to the equations: $\varepsilon_c = At^p = A_o\sigma t^p$, where ε_c is in %, t is in hours and σ is in GPa

Temperature (°C)	σ (MPa)	A (GPa^{-1}) (10^{-4})	A_o (10^{-4})	p	creep time (hrs)	creep strain (%)	recovery time (hrs)	recovered strain (%)
AIR								
1400	138	9.7	70.4	0.39	> 200	0.09	--	--
	207	12.8	62.0	0.36	100	0.10	--	--
	207	11.3	54.5	0.43	111	0.15	17.7	0.04
	276	12.5	45.2	0.44	41.4	0.13	--	--
	413	8.5	20.7	0.57	17.2	0.13	--	--
1535	103	18.8	183	0.59	13.6	0.07	24.4	0.03
	138	19.3	140	0.62	32.7	0.16	--	--
	276	17.2	62.3	0.72	7.4	0.15		
	276				3.6	0.14	0.9	0.05
	276				1.5	0.10	42.9	0.04
VACUUM								
1420	200	2.04	10.2	0.47	100	0.19	--	--
1510	200	4.20	21.0	0.53	100	0.50	--	--
1510	200	11.9	59.5	0.46	100	0.95	--	--
1600	200				16	1.02	47	0.12
	200	18.8	94.0	0.58	+ 30(46)	1.51	30	0.12
	200	29.0	145	0.39	120	1.68	--	--

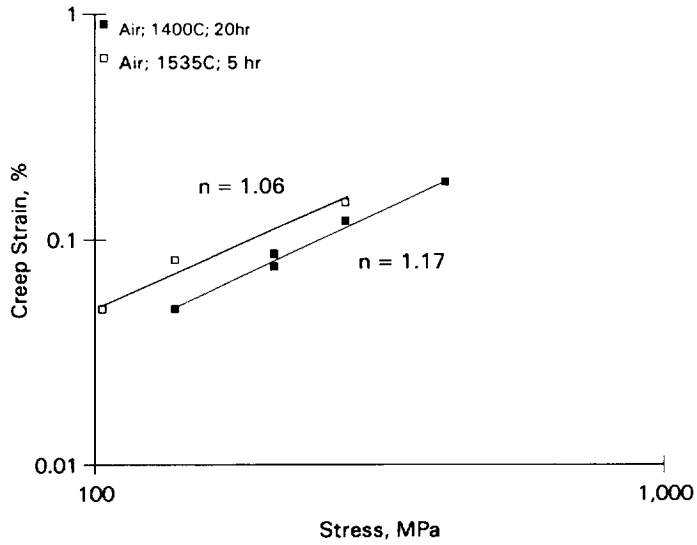

Figure 6. The stress dependence of creep strain measured in air after 20 hours at 1400°C and 5 hours at 1535°C.

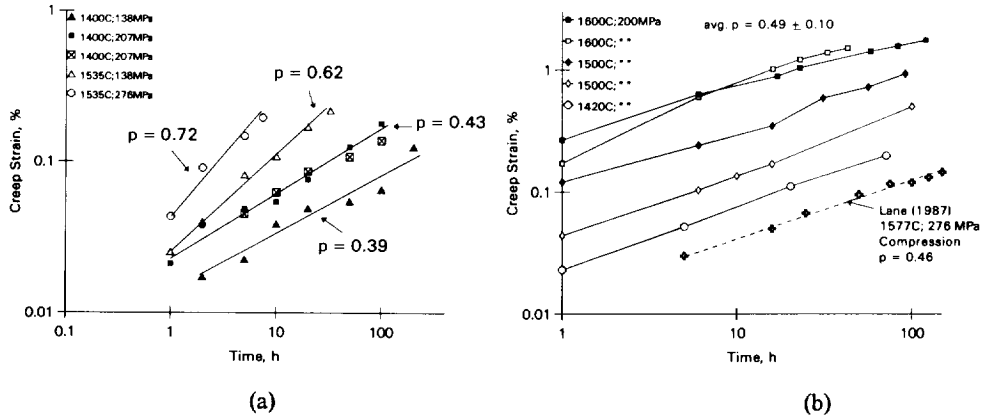

Figure 7. Tensile creep strain versus time for (a) air experiments at 138 and 207 MPa and (b) vacuum experiments at 200 MPa. The data from Lane (1987) in (b) is compression creep data for bulk α-SiC in argon at 276 MPa.

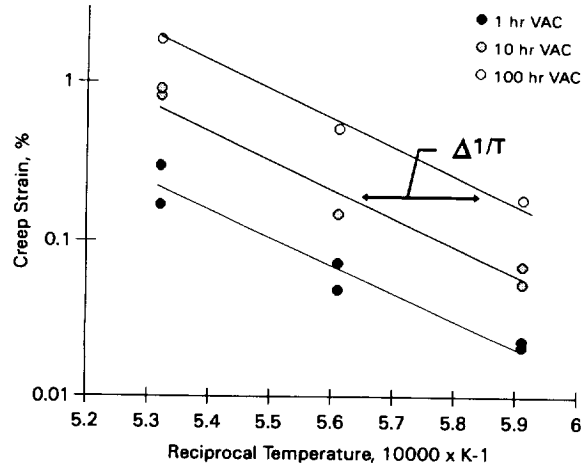

Figure 8. The creep strain at 1, 10, and 100 hours is plotted versus reciprocal temperature for 200 MPa vacuum creep experiments.

Comparing BSR and Tensile Creep

BSR data can be used to predict tensile creep data using simple linear viscoelastic principles assuming (1) that the stress dependence for creep is linear, (2) that creep in tension is equal in magnitude to creep in compression, and (3) that the controlling

mechanism are broadly distributed in relaxation times (Nowick and Berry, 1982). The first assumption has already been shown to be true for the experimental conditions of this study in tension creep and bend stress relaxation (m independent of applied bend strain). The second assumption is unknown and some studies have shown creep in tension to be greater than creep in compression for ceramics (e.g. Wiederhorn et al., 1988). The third assumption is reasonable for a large spectrum of grain boundary sliding events causing the overall deformation. Based on the above, it can be shown (Morscher et al., 1991 and DiCarlo and Morscher, 1991) that the predicted tensile creep strain $\varepsilon_{c(BSR)}$, can be related to the BSR m ratio by (2) where E is the elastic modulus.

$$\varepsilon_{c(BSR)} = [\sigma/E^{-1}]\{[1/(m(t)] - 1\} \qquad (2)$$

The BSR predicted creep strain (for 200 MPa) is plotted with 200 MPa vacuum creep data for the 1,10, and 100 hour tensile creep data in Fig. 9. Each m was converted to $\varepsilon_{c(BSR)}$, and the 10 and 100 hour data displaced to the 1 hour data via the linear regression technique. The apparant activation energy from $\Delta(1/T)$ was found to be 850 $\pm$ 50 kJ/mol. As can be seen from Fig. 9, the BSR predicted creep strain underestimates the actual tensile creep strain magnitude by about a factor of two, but has approximately the same time and temperature dependence as the tensile data. It is possible that creep (relaxation) in tension is, in fact, greater than creep (relaxation) in compression and is the reason for the underestimation of predicted creep strain magnitude from BSR data.

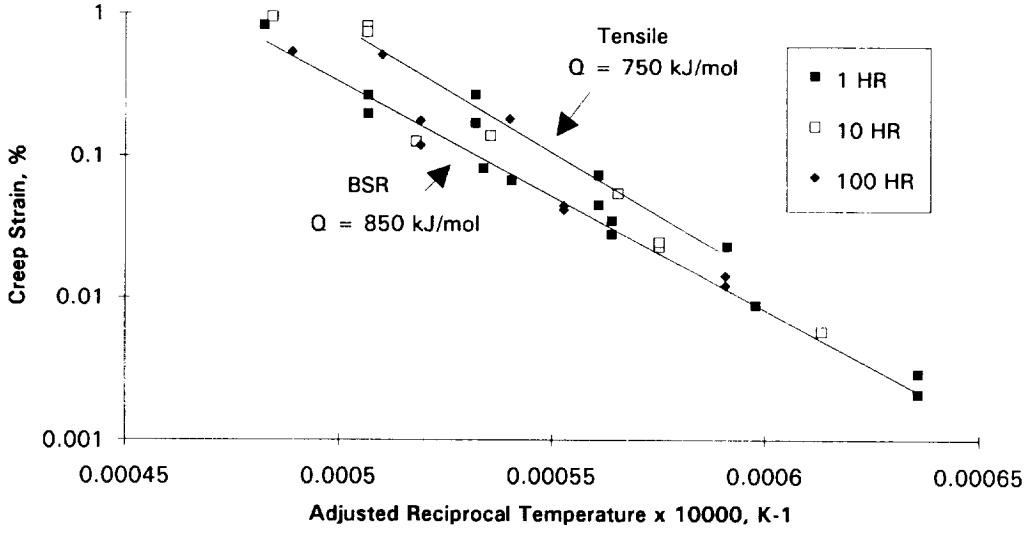

Figure 9. Tensile creep strain and predicted tensile creep strain from BSR data at 1, 10, and 100 hours for 200 MPa creep plotted vs. the adjusted (1 hour) reciprocal temperature.

BSR and Tensile Creep Recovery

The data for several tensile creep recovery experiments are shown in Fig. 5. The largest strain recovered was 0.12% for a 1600°C vacuum creep experiment where the total creep strain was 1.02% (Table I). Fig. 10 shows the tensile recovery strain normalized with maximum creep strain plotted versus the recovery time normalized by the

experimental tensile creep time. For the lower-temperature 0.1 to 0.2% creep strain experiments, as much as 40% of the strain was recovered. Only one creep recovery experiment (1535°C; 276 MPa) appeared to reach a maximum recovery strain after a recovery time of approximately 5 times the creep time. As creep strain is increased the magnitude of recovered strain increases but the ratio of recovered strain to maximum creep strain decreases.

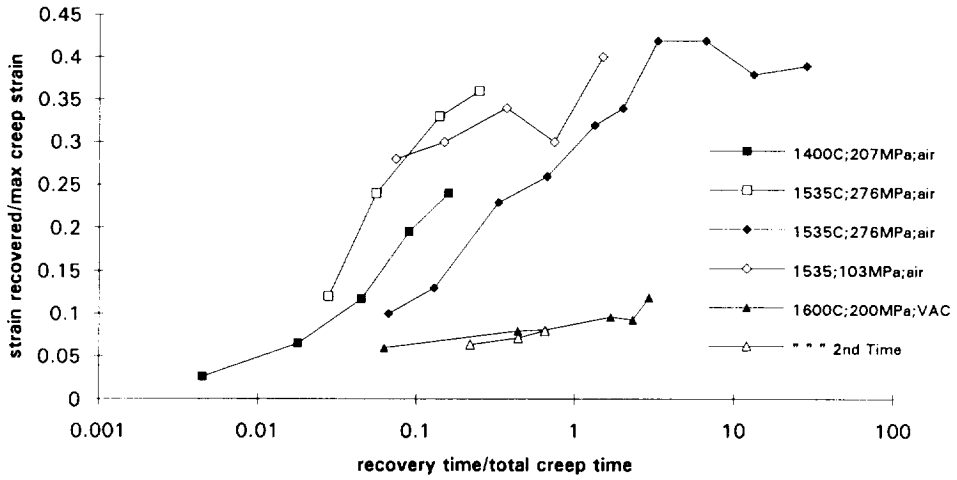

Figure 10. Typical tensile recovery data plotted as recovered strain normalized by maximum creep strain vs. recovery time normalized by total creep time.

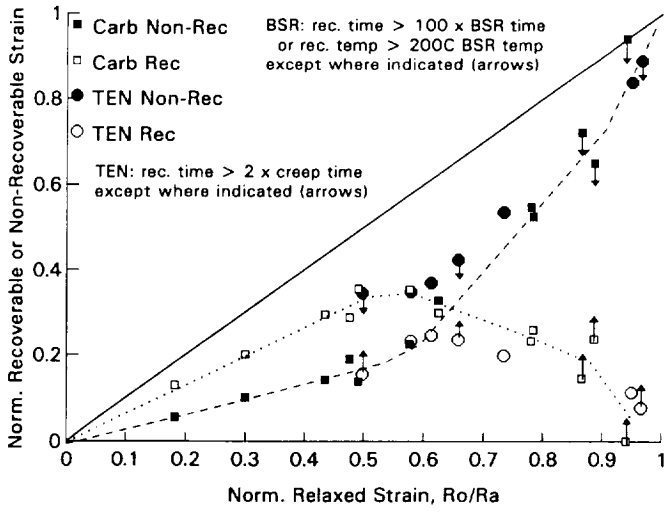

Figure 11. Recovered and non-recovered BSR strain normalized by applied strain, $\varepsilon_o = R_f/R_o$, plotted vs. the normalized relaxed strain (1-m).

The data for BSR strain recovery is shown in Fig. 11 as the normalized recovered (or anelastic) strain, $\mathcal{E}_a = R_o(R_a^{-1} - R_r^{-1})$,and normalized non-recovered (or viscous) strain, $\mathcal{E}_v = R_o/R_r$, versus the normalized relaxed (from BSR) strain, $\mathcal{E}_{BSR} = R_o/R_a$. If the fiber was fully anelastic or fully viscous, $\mathcal{E}_a$ or $\mathcal{E}_v$ would follow the line drawn on Fig. 11 with a slope of 1 for a given ε_{BSR}, respectively. Instead, the fiber, in bending, appears to have a greater anelastic component for $\mathcal{E}_{BSR} \leq 0.6$ ($m \geq 0.4$) above which the viscous component of the strain dominates. The data points with arrows signify that the recovery conditions were not 200°C greater and/or 2 orders of magnitude in time greater than the BSR conditions. Part of the anelastic component of strain may be due to creep in tension being greater than creep in compression. Also plotted on Fig. 11 are tensile recovery data (Table 1) converted (Eqn. 2) into BSR $\mathcal{E}_{BSR}$ (i.e. 1-m), $\mathcal{E}_a$ and $\mathcal{E}_v$. The tensile data underestimates the anelastic component of strain. This difference would account for about a factor of two (at the most) greater creep in tension than compression. However, the largest contribution of the anelastic component of strain (BSR) would be due to an internal mechanism and not the test configuration.

DISCUSSION

Compression creep studies have been performed on bulk α-SiC (Lane et al., 1988 and Nixon and Davis, 1992). In both of these studies, significant primary creep was observed in the same temperature, time and stress regimes as in this study. Compression creep data is shown in Fig. 7b from Lane (1987) for creep at 1577°C and 276 MPa. There appears to be similar time dependencies; however, the creep strain magnitude in compression is over an order of magnitude less than the tensile data. The α-SiC studied by Lane had a grain size of ~ 3.7 μm and contained some B and C in the form of B_4C precipitates within the grains. A near linear stress dependence (with creep strain rate) was also found at temperatures below 1650°C. In the bulk compression creep studies, a change in controlling activation energy (~ 450 kJ/mol below 1650°C to ~ 850°kJ/mol above 1650°C) was found from the steady state analysis. It was determined that grain boundary diffusion accommodated grain boundary sliding controls the low temperature regime and lattice diffusion accommodated grain boundary sliding in conjunction with some dislocation glide controls the high temperature creep.

Since the creep behavior of this study did not reach a steady state it is difficult to directly compare the results with the compressive creep work in the literature. However, the activation energies determined from both the higher activation energies found in the earlier studies and in this study are similar. This would infer lattice diffusion of C (714 kJ/mol, Hong and Davis, 1980) or Si (697 kJ/mol, Hong et al., 1981) as controlling the creep and relaxation.

The occurrence of primary creep for creep strains up to 2% was surprising. Primary creep could be due to several mechanisms. If creep is only due to diffusional mechanisms, grain growth would result in a decelerating creep rate as grain size increases as a function of time. However, this mechanism would not account for the build up of a back stress and resulting recovery upon removal of the stress at temperature. If a dislocation mechanism controls creep it could account for the occurrence of a primary creep region and the occurrence of creep recovery due to the dislocation density not reaching equilibrium. However, there would be a large stress dependence for creep which is not observed for the SiC studied here. A plausible explanation for at least part of the primary creep and creep recovery is the build-up of elastic stress in the grains as a result of grain boundary sliding. This mechanism (Zener, 1941 and Ke, 1947) is described by the

grain boundary having a viscosity and the grains deforming elastically to accommodate the deformation. If this were the case, the elastic strain capable of being accommodated would be on the order of the applied elastic strain from the models of Zener (1941), Ke (1947), and Raj and Ashby (1971). The maximum creep strain recovered in this study was 0.12%. If E was 320 GPa at 1600°C (Fukuhara and Abe, 1993), the calculated elastic strain would be ~0.06% or half the strain recovered. In other words, the maximum strain recovered would be greater than the strain predicted from the models mentioned. Therefore the simple models of elastic accommodation of strain do not explain the magnitude of strain recovered.

SUMMARY AND CONCLUSIONS

The time dependent deformation in bending (constant strain) and tension (constant load) have been determined for α-SiC fibers between 1300 and 1800°C for bending experiments and between 1400 and 1600°C for tensile experiments. Similar activation energies were determined from argon BSR data (850 kJ/mol) and vacuum tensile data (750 kJ/mol) which infer creep and relaxation are both controlled by lattice diffusion of C or Si. Steady state creep was never reached for the tensile creep experiments, even up to 2% creep strain. Simple viscoelastic principles were used to predict tensile creep from BSR data. BSR data underestimated the tensile creep strain by about a factor of 2, but predicted approximately the same time and temperature dependence. The difference in magnitude, at least partially, was attributed to creep in compression being less than creep in tension. BSR and tensile recovery experiments showed significant recovery of strain, infering a mechanism for creep capable of building up a back stress such as grain boundary sliding accommodated by elastic deformation of the grains. However, the amount of strain recovered would be greater than expected from elastic accommodation by grain boundary sliding.

ACKNOWLEDGEMENTS

The authors would like to thank Prof. James Cawley of CWRU, Dr. John D. Whittenberger of NASA Lewis, and Dr. James DiCarlo for useful discussions and review of the manuscript.

REFERENCES

Damask, A.C. and Dienes, G.J., "Point Defects in Metals," Gordon and Breach, NY (1963).

DiCarlo, J.A., 1994, Creep limitations of current polycrystalline ceramic fibers, *Comp. Sci. Tech.*, 51:213.

DiCarlo, J.A. and Morscher, G.N., 1991, Creep and stress relaxation modeling of polycrystalline ceramic fibers, in: "Failure Mechanisms in High Temperature Composite Materials," 1991 Winter Annual Meeting of ASME, Atlanta, Georgia, Dec. 1-6, 1991. p. 15.

Frechette, F., Dover, B., Venkateswaran, V, and Kim, J., 1991, High temperature continuous sintered SiC fiber for composite applications, *Ceram. Eng. Sci. Proc.*, 12:992.

Fukuhara, M. and Abe, Y., 1993, High-temperature elastic moduli and internal frictions of α-SiC ceramic, *J. Mater. Sci. Let.*, 12:681.

Giannuzzi, L., private communication.

Goldsby, J., Yun, H.M. Yun, and DiCarlo, J.A., Creep and rupture strength of an advanced CVD SiC fiber, to be published as a NASA TM.

Hong, J.D. and Davis, R.F., 1980, Self-diffusion of carbon-14 in high purity and n-doped α-SiC single crystals, *J. Am. Ceram. Soc.*, 63:546.

Hong, J.D., Newberry, D.E., and Davis, R.F., 1981, Self-diffusion of ^{30}Si in α-SiC single crystals, *J. Mater. Sci.*, 16:2485.

Ke, T.S., 1947, Experimental evidence of the viscous behavior of grain boundaries in metals, *Phys. Rev.*, 71:533.

Lane, J.E., 1987, Kinetics and Mechanisms of Primary and Steady-State Creep in Sintered Alpha Silicon-Carbide, PhD Thesis, North Carolina State University, 111.

Lane, J.E., Carter, C.H. Jr., and Davis, R.F., 1988, Kinetics and mechanisms of high-temperature creep in silicon carbide: III, sintered α-silicon carbide, *J. Am. Ceram. Soc.*, 71:281.

Morscher, G.N. and DiCarlo, J.A., 1992, A simple test for thermomechanical evaluation of ceramic fibers, *J. Am. Ceram. Soc.* 75:136.

Morscher, G.N., DiCarlo, J.A., and Wagner, T., 1991, Fiber creep evaluation by stress relaxation measurements, *Ceram. Eng. Sci. Proc.*, 12:1032.

Nowick, A.S. and Berry, B.S, 1982, "Anelastic Relaxation in Crystalline Solids", Academic Press, NY.

Nixon, R.D. and Davis, R.F., 1992, Diffusion-accommodated grain boundary sliding and dislocation glide in the creep of sintered alpha silicon carbide, *J. Am. Ceram. Soc.*, 75:1786.

Raj, R. and Ashby, M.F., 1971, On grain boundary sliding and diffusional creep, *Met. Trans.* 2:1113.

Sherby, O.D. and Dorn, J.E., 1952, Creep correlations in alpha solid solutions of aluminum, *Trans. AIME*, 194:959.

Sherby, O.D., Orr, R.L., and Dorn, J.E., Creep correlations of metals at elevated temperatures, *Trans. AIME*, 200:71.

Wiederhorn, S.M., Roberts, D.E., Chuang, T-J., and Chuck, L., 1988, Damage-enhanced creep in siliconized silicon carbide: phenomenology, *J. Am. Ceram. Soc.*, 71:602.

Yun, H.M., Goldsby, J., and DiCarlo, J.A., 1994, Tensile creep and stress-rupture behavior of polymer derived SiC fibers, NASA TM 106692.

Zener, C., 1941, Theory of the elasticity of polycrystals with viscous grain boundaries, *Phys. Rev.*, 60:906.